Supplementary Information

Control of associative learning by the mediodorsal thalamus-orbitofrontal cortex circuit

Ziwei Le, Can Huang, Wen Zhang, Jingyu Ren, and Haishan Yao

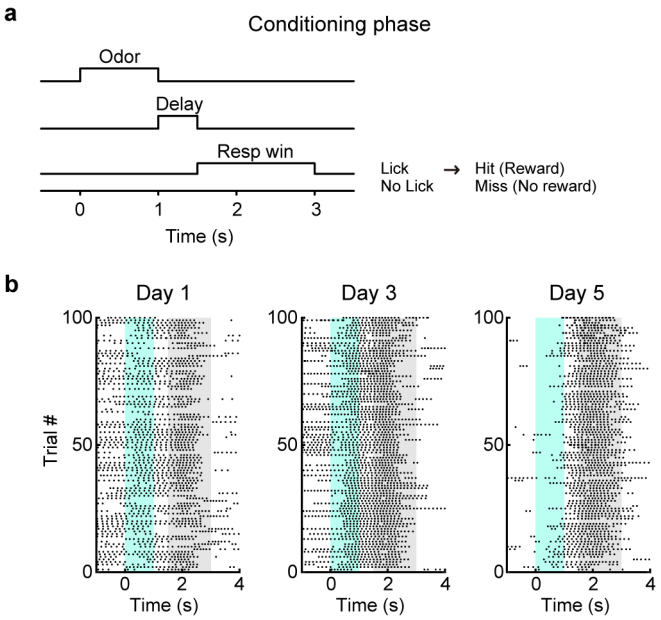

Supplementary Figure 1 | Conditioning phase to establish reward expectation following odor cue.

a Schematic of the trial structure during the conditioning phase. **b** Lick raster of an example mouse in three conditioning sessions. Cyan shading, odor cue presentation; gray shading, response window.

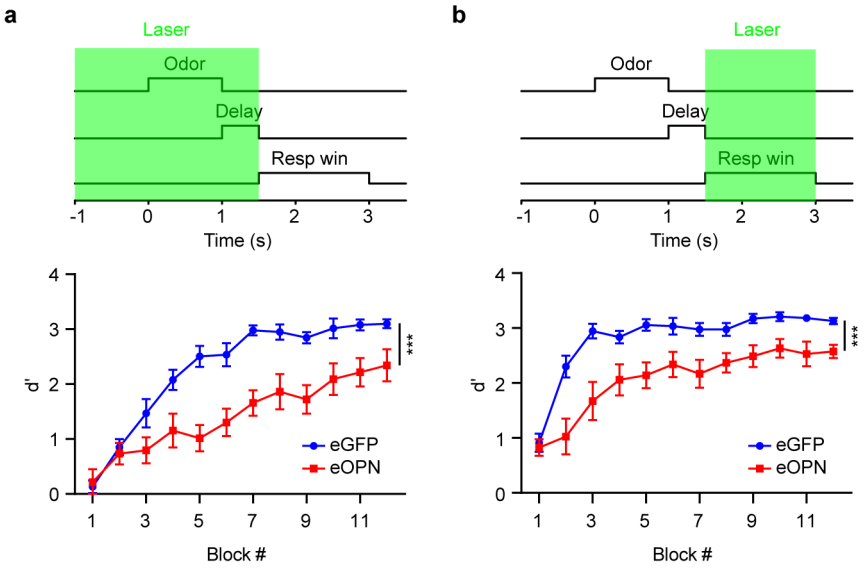

Supplementary Figure 2 | The activity of MD projections to OFC during both cue-delay period and response window is crucial for learning.

a Inactivation of MD projections to OFC from -1 to 1.5 s relative to odor cue onset (covering cue-delay period) impaired discrimination learning ($F_{(1, 19)}$ = 16.78, ***p = 6.14×10^{-4}, two-way ANOVA with mixed designed; eGFP mice: n = 11, eOPN mice: n = 10). **b** Inactivation of MD projections to OFC from 1.5 to 3 s relative to odor cue onset (covering response window) impaired discrimination learning ($F_{(1, 18)}$ = 18.23, ***p = 4.61×10^{-4}, two-way ANOVA with mixed designed; eGFP mice: n = 10, eOPN mice: n = 10). For both **a** and **b**, 20 trials/block. Error bars, mean ± s.e.m.

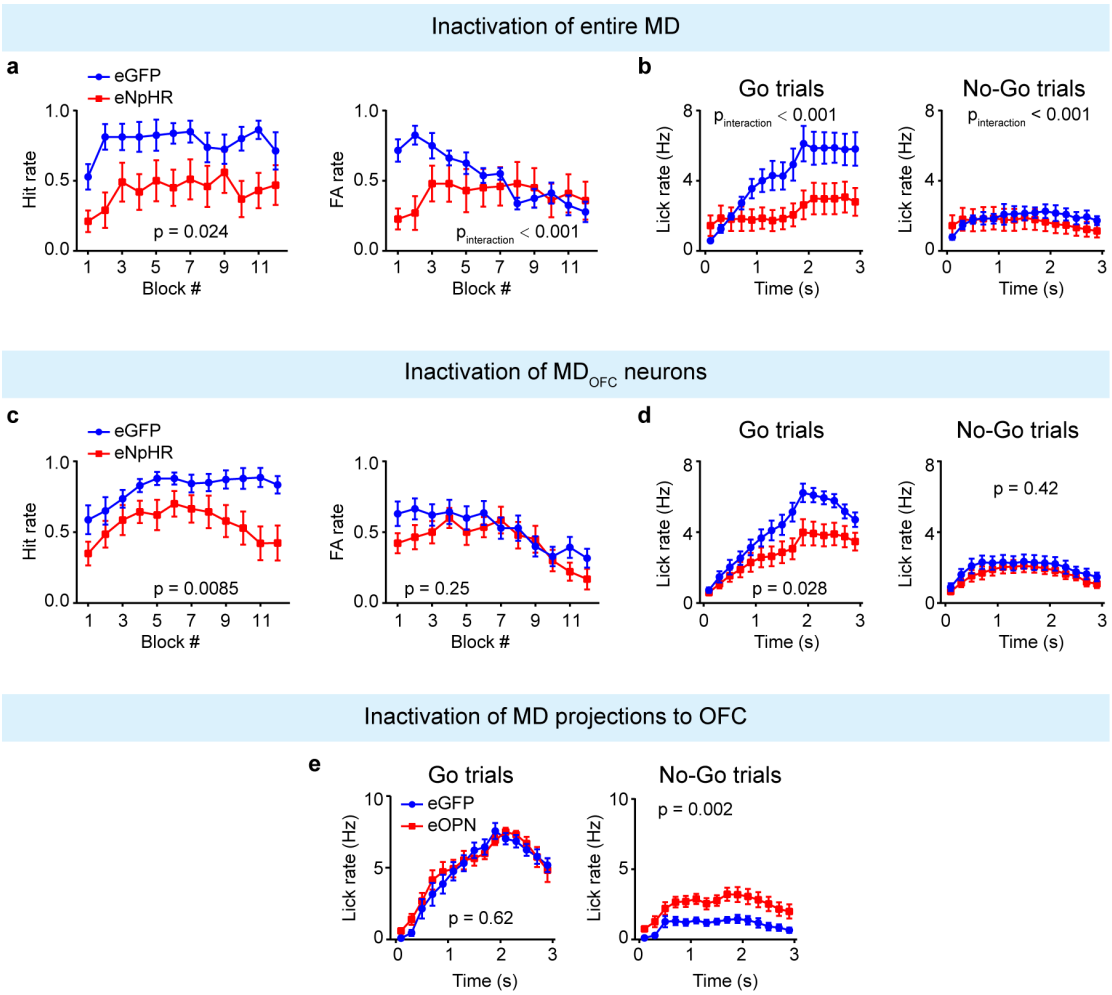

Supplementary Figure 3 | Inactivation of the entire MD or MD$_{OFC}$ neurons impairs learning and licking motivation.

a Effect of entire MD inactivation on Hit rate and FA rate (eGFP mice: n = 8, eNpHR mice: n = 10). **b** Inactivation of the entire MD significantly reduced lick rate in Go trials. **c** Effect of inactivating MD$_{OFC}$ neurons on Hit rate and FA rate (eGFP mice: n = 14, eNpHR mice: n = 14). **d** Inactivation of MD$_{OFC}$ neurons significantly reduced lick rate in Go trials. **e** Inactivation of MD projections to OFC did not affect lick rate in Go trials (eGFP mice: n = 11, eOPN mice: n = 10). Two-way ANOVA with mixed designed. For **a** and **c**, 20 trials/block. Error bars, mean ± s.e.m.

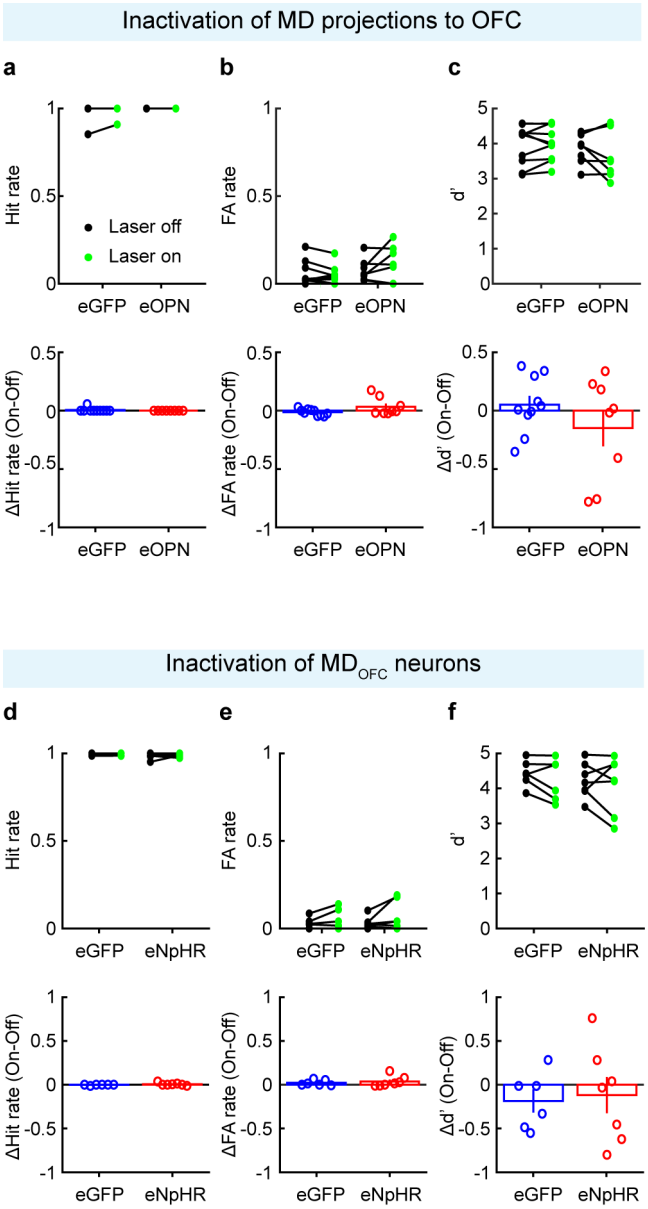

Supplementary Figure 4 | Inactivation of the entire MD or MD_{OFC} neurons does not affect performance in well-trained mice.

a−c Inactivation of the entire MD did not affect Hit rate, FA rate or d′. eGFP mice: n = 10, eOPN mice: n = 8. $p > 0.05$, **d−f** Inactivation of MD_{OFC} neurons did not affect Hit rate, FA rate or d′. eGFP mice: n = 6, eNpHR mice: n = 7. $p > 0.05$, Wilcoxon rank-sum test was used to compare eGFP and eOPN mice. Error bar denotes ± s.e.m.

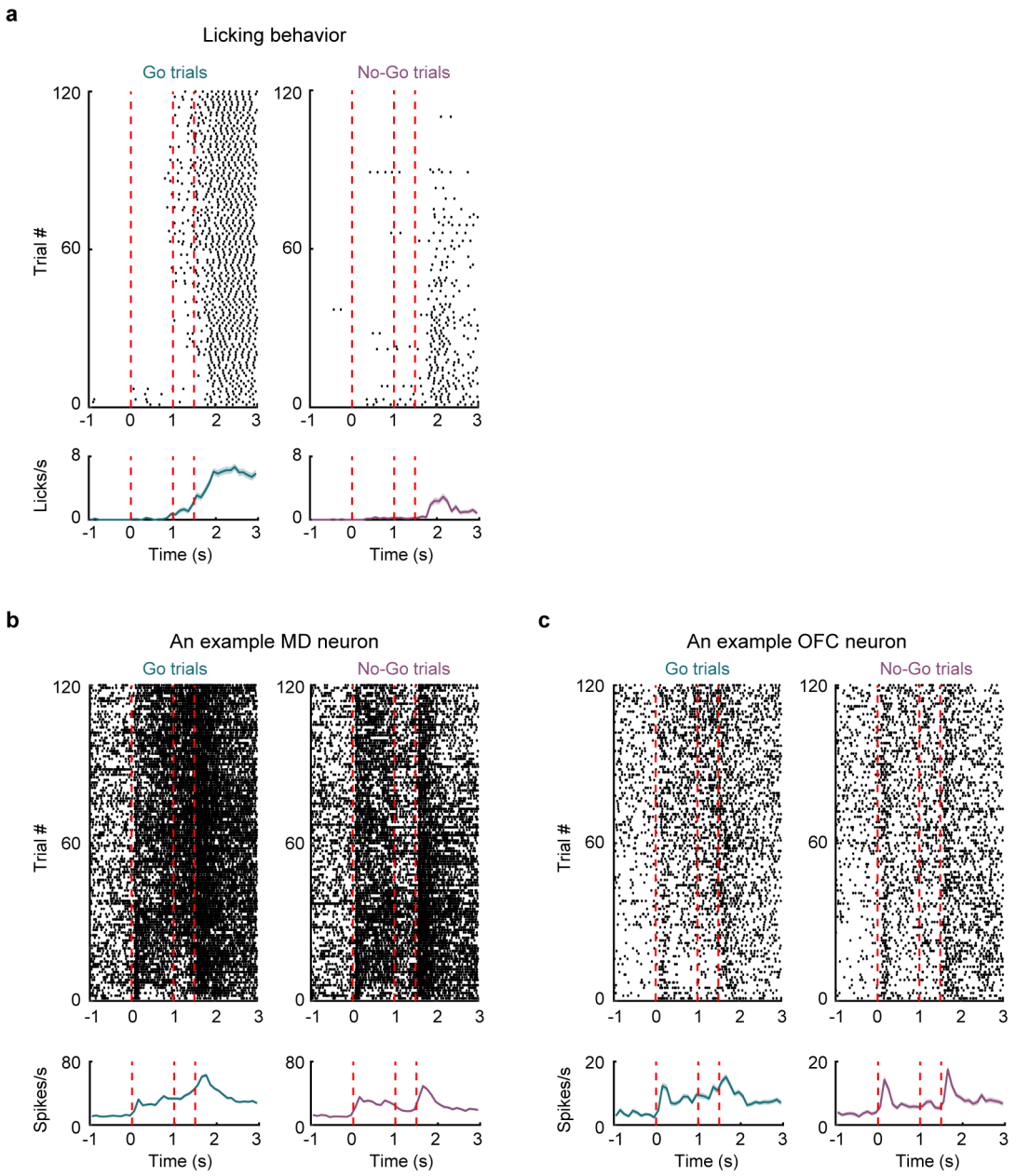

Supplementary Figure 5 | Responses of example MD and OFC neurons during discrimination learning.

a Lick raster and lick PSTHs in Go and No-Go trials. The first, second, and third vertical dashed lines indicate odor cue onset, odor cue offset, and response window onset, respectively. **b** Spike raster and PSTHs for an example MD neuron in Go and No-Go trials. **c** Spike raster and PSTHs for an example OFC neuron in Go and No-Go trials. Shaded areas in PSTHs indicate s.e.m.

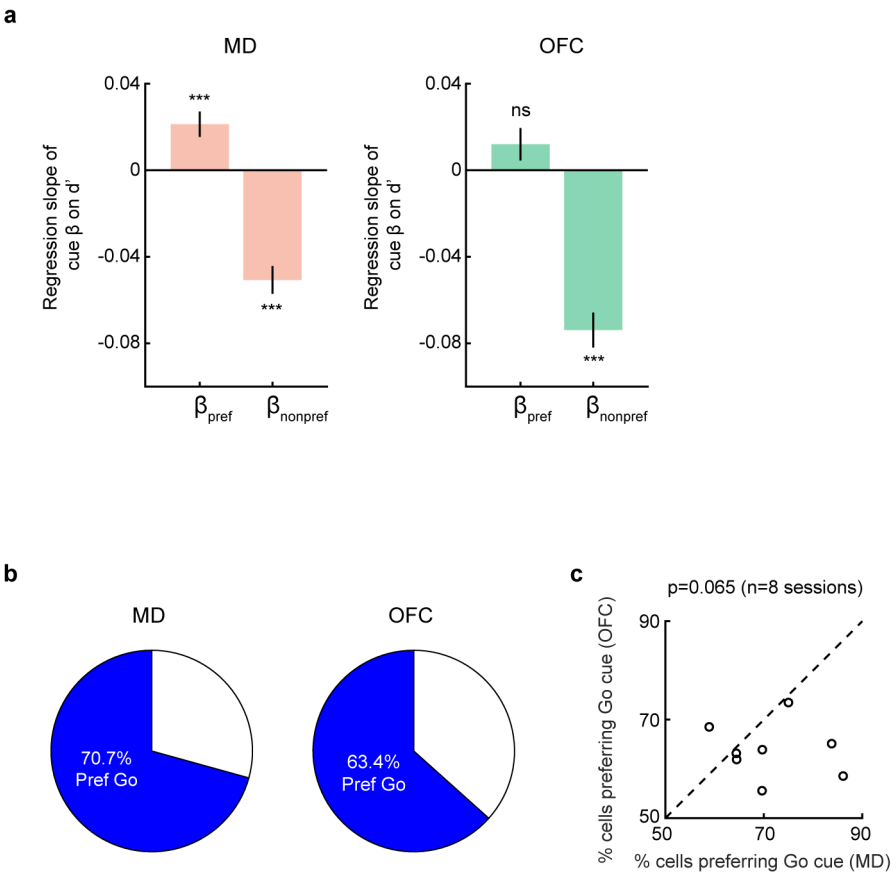

Supplementary Figure 6 | Regression slope of cue β on d' and proportion of neurons selective for the odor cue in Go trials.

a Left, regression slope of β_{pref} (***p = 1.72×10^{-5}) or $\beta_{nonpref}$ (***p = 4.65×10^{-13}) on d′ for MD neurons (n = 471). Right, same as left, but for OFC neurons (n = 415, ***p = 3.01×10^{-17}). Wilcoxon signed-rank test. **b** Proportion of MD and OFC neurons preferring the odor cue in Go trials at the end of discrimination learning. **c** Session-wise comparison of the proportion of such neurons in MD and OFC. p = 0.065, n = 8 sessions, Wilcoxon signed-rank test.

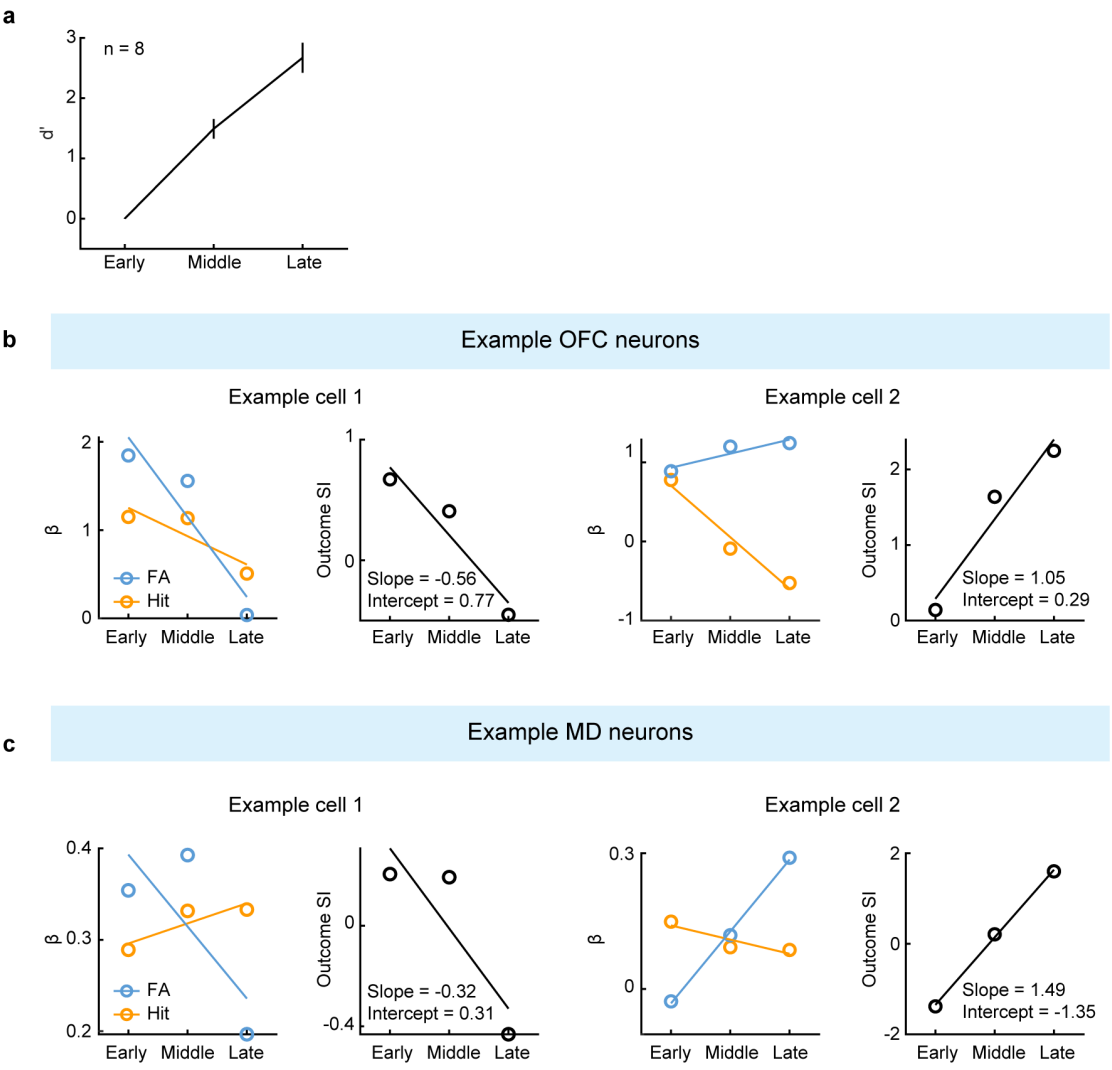

Supplementary Figure 7 | Linear regression of outcome β or outcome SI across learning phases for example neurons.

a d′ across the three learning phases in mice used for neuropixels recordings (n = 8 sessions). Error bars, mean ± s.e.m. **b** Two example OFC neurons showing changes in β_{FA}, β_{Hit}, and outcome SI across the three learning phases. **c** Two example MD neurons showing changes in β_{FA}, β_{Hit}, and outcome SI across the three learning phases.

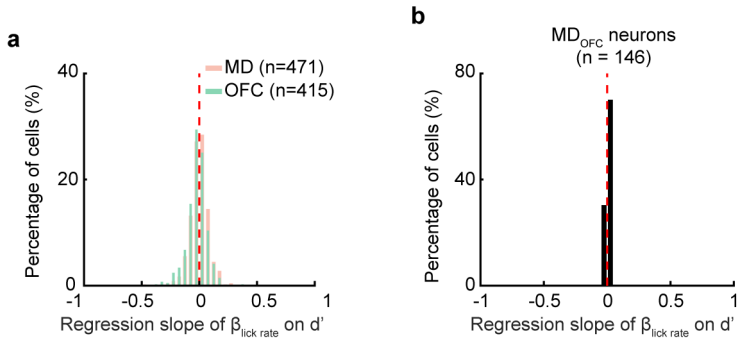

Supplementary Figure 8 | Linear regression of $\beta_{\text{lick rate}}$ against d′.
a Distributions of regression slope of $\beta_{\text{lick rate}}$ on d′ for MD and OFC neurons. The mean slope is close to zero in both regions. **b** Same as **a**, but for MD_{OFC} neurons.

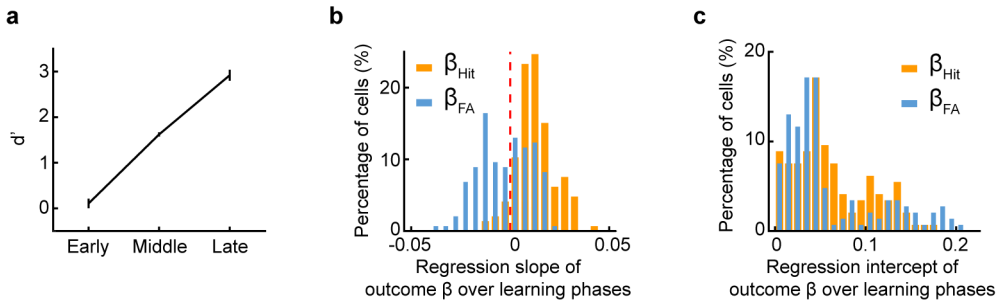

Supplementary Figure 9 | Regression slope and intercept of outcome β across learning phases for MD$_{OFC}$ neurons.

a d′ across the three learning phases in mice used for calcium imaging of MD$_{OFC}$ neurons (n = 9 sessions). **b** Distribution of regression slope of β_{FA} ($p = 0.0015$) and β_{Hit} ($p = 1.34\times10^{-21}$). **c** Distribution of regression intercept of β_{FA} ($p = 1.04\times10^{-25}$) and β_{Hit} ($p = 1.04\times10^{-25}$). n = 146 neurons, Wilcoxon signed-rank test. Error bars, mean ± s.e.m.

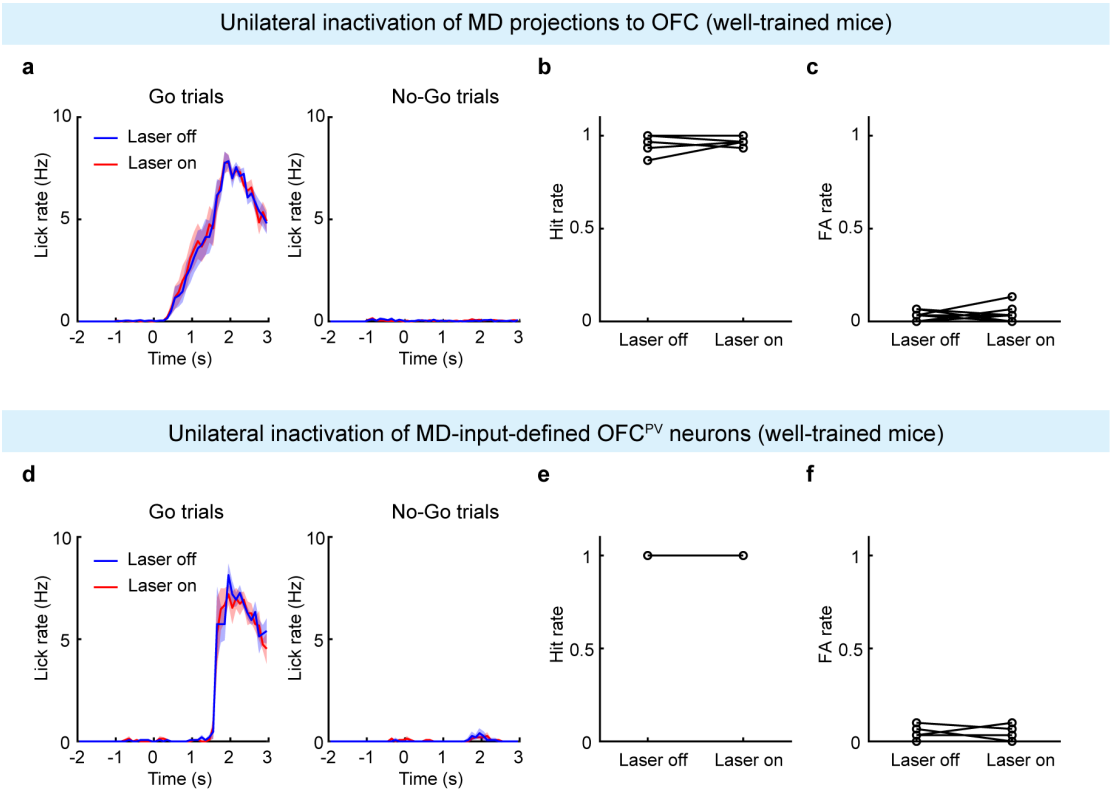

Supplementary Figure 10 | Effect of laser stimulation on performance in well-trained mice used for electrophysiological experiments.

a–c Unilateral inactivation of MD projections to OFC did not affect lick rate, Hit rate, or FA rate in well-trained mice (n = 15 sessions). **d–f** Unilateral inactivation of MD-input-defined OFC^{PV} neurons similarly had no effect on lick rate, Hit rate, or FA rate in well-trained mice (n = 5 sessions).

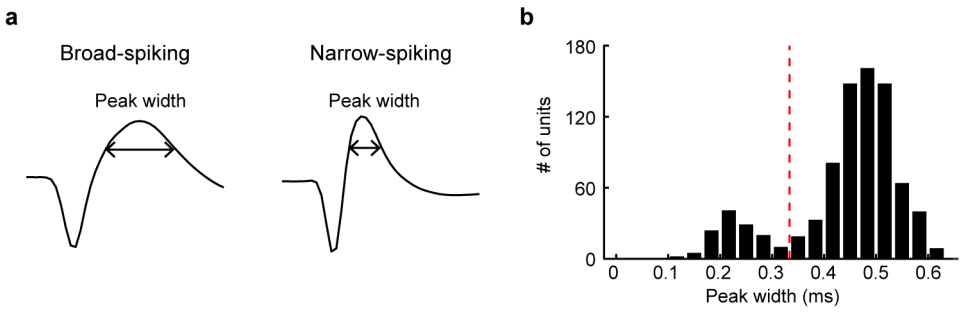

Supplementary Figure 11 | Spike waveforms of OFC neurons.
a Example spike waveforms illustrating peak width for a broad-spiking and a narrow-spiking cell. **b** Distribution of peak widths across the OFC neuron population. Neurons with peak widths < 0.33 ms were classified as narrow-spiking, and those with peak widths $\geqslant$ 0.33 ms as broad-spiking.

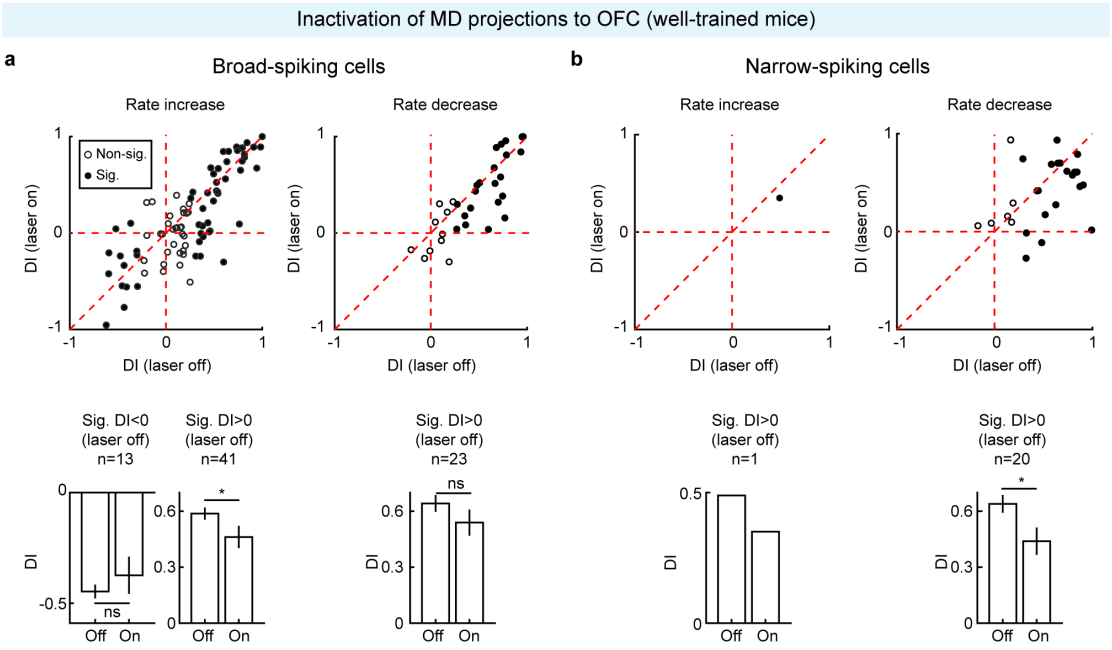

Supplementary Figure 12 | Effect of inactivating MD projections on DI of OFC broad-spiking and narrow-spiking cells in well-trained mice.

a Top, DI under laser-on versus laser-off conditions for OFC broad-spiking cells that showed significantly increased firing rates (left) or decreased firing rates (right) upon MD projections inactivation. Bottom, among neurons with significantly increased firing rate, DI magnitude was significantly reduced in those exhibiting a significant positive DI under the laser-off condition (*p = 0.02, n = 41, Wilcoxon signed-rank test). **b** Top, DI under laser-on versus laser-off conditions for OFC narrow-spiking cells that showed significantly increased firing rate (left) or decreased firing rate (right). Bottom, among neurons with significantly decreased firing rate, DI magnitude was significantly reduced in those exhibiting a significant positive DI under the laser-off condition (*p = 0.016, n = 20, Wilcoxon signed-rank test). Solid circles, neurons with significant DI ($p < 0.05$) under the laser-off condition.

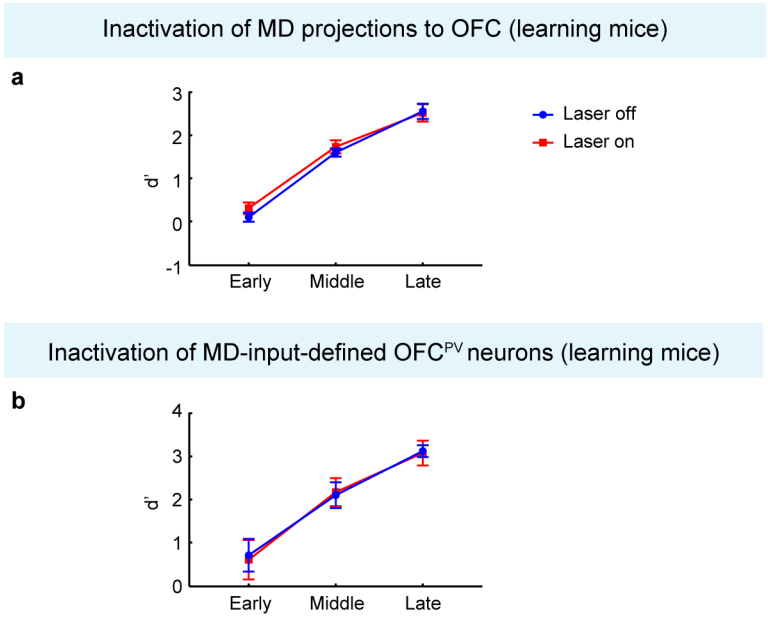

Supplementary Figure 13 | Effect of laser stimulation on performance in learning mice used for electrophysiological experiments.

a Unilateral inactivation of MD projections to OFC did not affect learning (n = 6 sessions). **b** Unilateral inactivation of MD-input-defined OFC^{PV} neurons did not affect learning (n = 4 sessions).

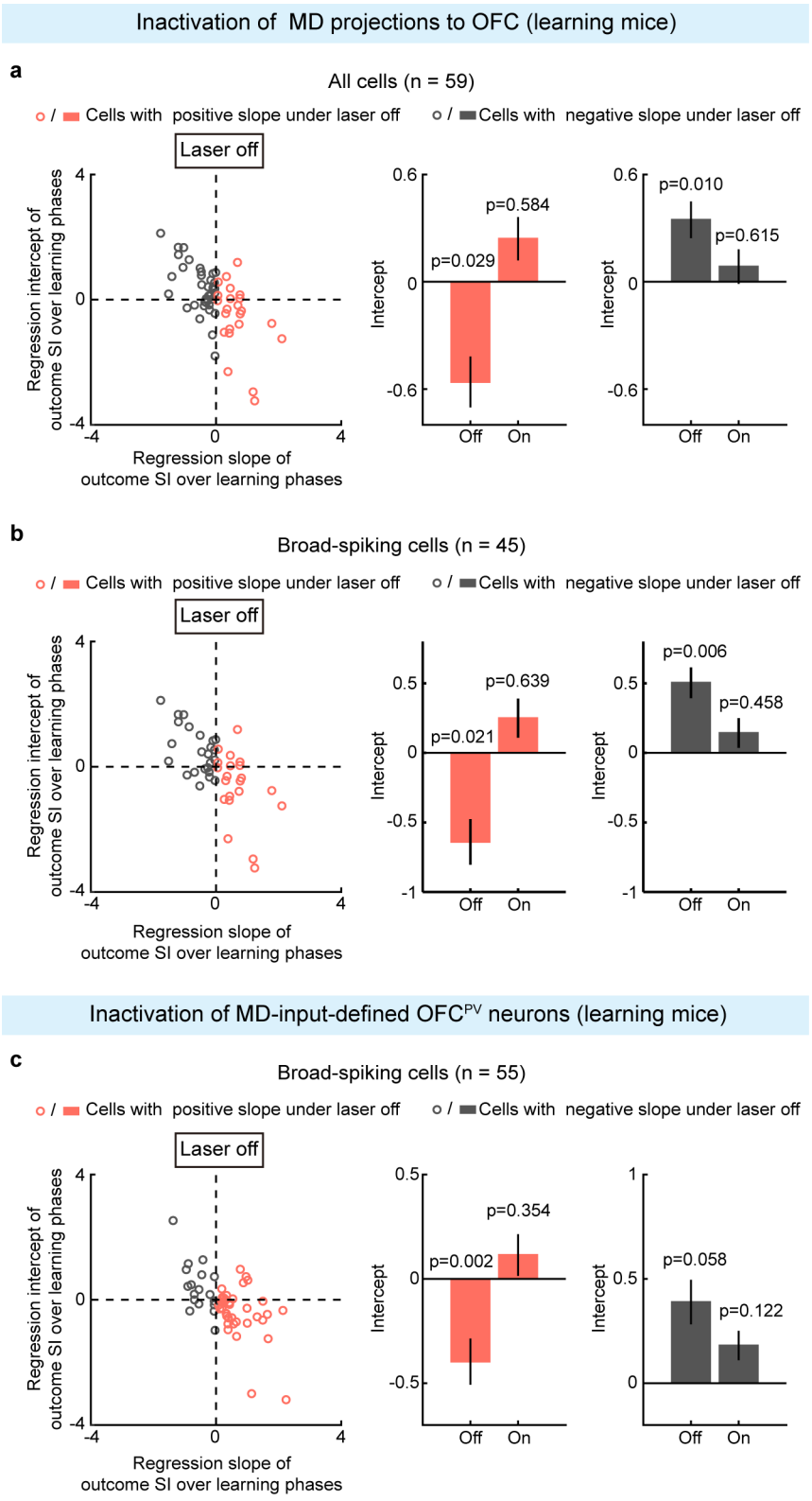

Supplementary Figure 14 | Effect of laser stimulation on the intercept of linear regression for outcome SI across learning phases.

a Left, scatter plot showing regression intercept versus slope of outcome SI across learning phases for OFC neurons (n = 59) under the laser-off condition during unilateral inactivation of MD projections to OFC. Middle, mean intercepts in laser-off condition

(p = 0.029) and laser-on condition (p = 0.584) for neurons with positive outcome SI slopes under the laser-off condition (n = 23). Right, same as middle, but for neurons with negative outcome SI slopes under the laser-off condition (n = 36). **b** Same as **a**, but for OFC broad-spiking cells. Left, n = 45. Middle, n = 21, Right, n = 24. **c** Left, scatter plot showing regression intercept versus slope of outcome SI across learning phases for OFC broad-spiking cells (n = 55) under the laser-off condition during unilateral inactivation of MD-input-defined OFC^{PV} neurons. Middle, mean intercepts in laser-off condition (p = 0.002) and laser-on condition (p = 0.354) for broad-spiking cells with positive outcome SI slopes under the laser-off condition (n = 37). Right, same as middle, but for neurons with negative outcome SI slopes under the laser-off condition (n = 18). Wilcoxon signed-rank test. Error bars, mean ± s.e.m.

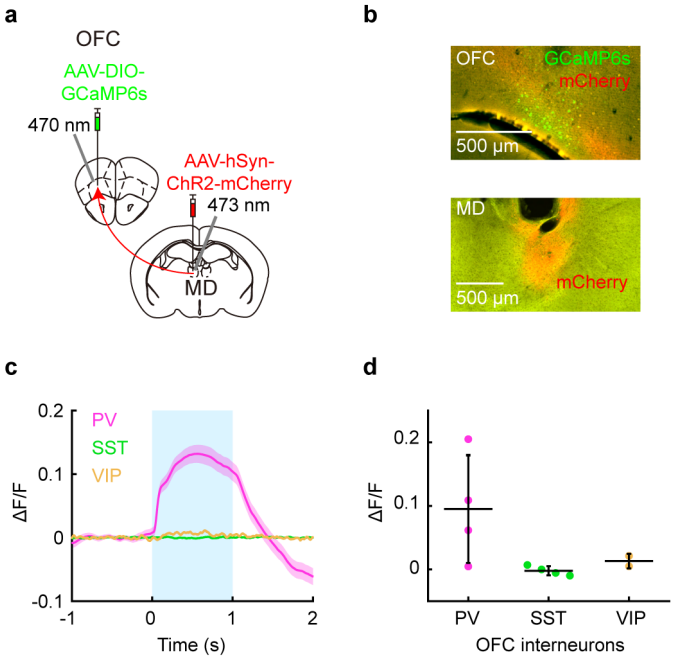

Supplementary Figure 15 | Effect of MD neuron activation on the in vivo responses of OFC interneurons.

a Schematic of virus injections into the MD and OFC, and optic fiber implantations over both regions in PV-Cre, SST-Cre, or VIP-Cre mice. **b** Representative fluorescence images showing the GCaMP6s expression in the OFC (top) and ChR2-mCherrey expression in the MD (bottom) for an example PV-Cre mouse. **c** Representative ΔF/F calcium signals in response to MD stimulation (blue shading) recorded from a PV-Cre, SST-Cre, and VIP-Cre mouse, respectively. **d** Peak ΔF/F amplitudes across cell types. PV-Cre: n = 4. SST-Cre: n = 4; VIP-Cre, n = 2. Error bars, mean ± s.e.m.